

Results of the Application of the Mdn in the Improvement of the Design of an Electrical Furnace that produces Low Carbon Ferromanganese

Jose P. SANCHO,¹⁾ Érika MARINAS,¹⁾ Miguel Ángel BARBÉS,¹⁾ Luis Felipe VERDEJA,¹⁾ Iñigo RUIZ-BUSTINZA,²⁾ Javier MOCHÓN²⁾ and Ramón Martín DUARTE²⁾

1) Group of Investigation in Iron and Steel Industry, Metallurgy and Materials, School of Mines, University of Oviedo, Calle Independencia s.n 33004 Oviedo Spain. 2) Centro Nacional de Investigaciones Metalúrgicas (CSIC/CENIM), Avda. Gregorio del Amo, 8, 28040-Madrid, Spain. E-mail: jmochon@cenim.csic.es

(Received on June 1, 2009; accepted on December 2, 2009)

Improvements developed in an electric furnace design for the production of refined ferromanganese (low carbon ferromanganese), using the Nodal Wear Model (NWM), are detailed in this paper.

Likewise, the NWM can be used as an instrument which is able to simulate situations that have not yet been carried out on industrial scale and to predict, for example, the performance of the electric furnace lining, under operational conditions that could form a cold wall/bottom.

Finally, the NWM has been applied to simulate and predict (refractory repair consumption) the operations of patching or hot repair during the furnace campaign.

KEY WORDS: refined ferromanganese; Nodal Wear Model (NWM); design; simulation.

1. Introduction

World-wide steel production is currently about 1 350 million tons per year (more specific, in the 2007 the production has been the 1 343 million tons). The 45% of total production is low carbon steels (ferritic steels), products ($C < 0.10\%$) while 25%, 10% and 20% of the rest, respectively, can be attributed to ferritic-pearlitic steels ($C = 0.25\%$), pearlitic steels ($C = 0.80\%$) and special products (stainless and high alloy).

Manganese has always been one of the common elements in the chemical specifications, both for carbon steels as well as for special steels. Nevertheless, and due to the importance of high resistance and high toughness ferritic products, its role as an alloy element has become highly valued in recent years. The presence of manganese in ferritic steel simultaneously favors resistance (σ_y , yield strength) as well as toughness (ITT °C, Impact Transition Temperature) of the products, a circumstance that is quite uncommon both in alloy elements of either a substitutional or interstitial solid solution character.

In the new generations of IF (Interstitial Free) steels it can be said that the role of carbon and of interstitial elements (nitrogen, hydrogen and boron) have been relegated to the category of impurity. The presence of the mentioned elements, however, remarkably diminishes the toughness of the product. For this reason one tends to value the contents in carbon and nitrogen that accompany the commercially used ferromanganese in the manufacture of ferritic steels. Recently, markets for electrolytic and low carbon ferroman-

gane qualities are being opened that were unimaginable just a few years ago.

The qualities of commercial ferromanganese (Fe–75%Mn) can reach carbon contents on the order of 2.0%. For low carbon ferromanganese, qualities with carbon contents below 1.0% are being demanded. However, as it is necessary to use a new reducer (Fe–55%Mn–20%Si) to achieve this level different a metallurgical coke, it has been necessary confront having to count on the presence of silicon (from 0.30 to 0.80% of Si) in the end product (refined ferromanganese with $\%C < 1\%$).¹⁾

The metallurgical importance of manganese can be verified by the data facilitated by the International Manganese Institute that considers annual production of said mineral to be in the neighborhood of 20 million tons (16 million expressed as manganese metal). Taking these figures into account, manganese would occupy the fourth position among metallic materials most used by humanbeing, only being surpassed by iron, aluminum and copper. The 90% of manganese production goes to the iron and steel industry and the rest is used as an alloy element in nonferrous metals.²⁾

2. Termal Characteristics of a Furnace

The manufacture of refined low carbon ferromanganese was carried out in an electrical furnace up until the year 2000, whose lining furnace was designed in agreement with the disposition of materials as indicated in **Fig. 1** and **Table 1**. The average coating life, before beginning a total reconstruction of the wall-plate and the bottom furnace is under-

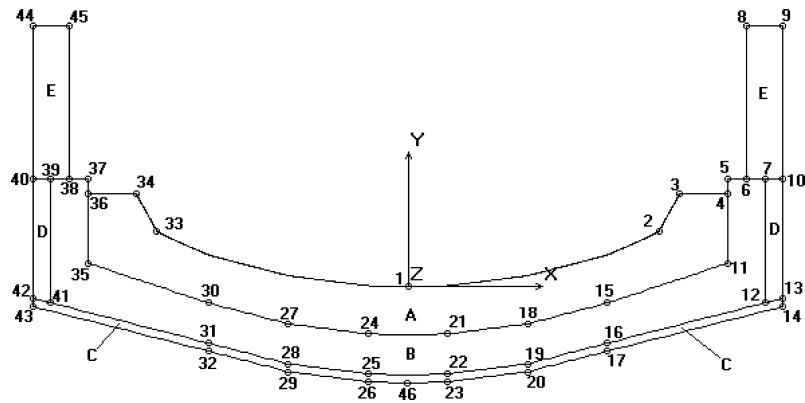


Fig. 1 Chemical, Table 1, geometrical and lining characteristics (regions A; B; C; D and E) of electric furnace according model M(18; 5.0; 14–19) to producing refined ferromanganese.

Table 1. Chemical (in mass%), geometrical and lining characteristics of electric furnace of the Fig. 1, according model M(18; 5.0; 14–19) to producing refined ferromanganese.

Region A: Magnesia castable refractory (MgO + CaO = 95%; SiO ₂ = 0.60%; Fe ₂ O ₃ = 3.8%; Al ₂ O ₃ = 0.30%) Thickness = 30 cm Region B: Brick Magnesia Sintered (Dense) Thickness = 25 cm Region C: Aluminous castable refractory (Monolithic Fireclay) Thickness = 5 cm Region D: Brick Chrome - Magnesia.					
Point	X coordinate	Y coordinate	Point	X coordinate	Y coordinate
1	0.00	0.00	24	-0.25	-0.29
2	1.57	0.35	25	-0.25	-0.54
3	1.70	0.58	26	-0.25	-0.59
4	2.00	0.58	27	-0.75	-0.23
5	2.00	0.68	28	-0.75	-0.48
6	2.12	0.68	29	-0.75	-0.53
7	2.24	0.68	30	-1.25	-0.10
8	2.12	1.63	31	-1.25	-0.35
9	2.35	1.63	32	-1.25	-0.4
10	2.35	0.68	33	-1.57	-0.35
11	2.00	0.15	34	-1.70	0.58
12	2.24	-0.10	35	-2.00	0.15
13	2.35	-0.07	36	-2.00	0.58
14	2.35	-0.12	37	-2.00	0.68
15	1.25	-0.10	38	-2.12	0.68
16	1.25	-0.35	39	-2.24	0.68
17	1.25	-0.4	40	-2.35	0.68
18	0.75	-0.23	41	-2.24	-0.10
19	0.75	-0.48	42	-2.35	-0.07
20	0.75	-0.53	43	-2.35	-0.12
21	0.25	-0.30	44	-2.35	1.63
22	0.25	-0.54	45	-2.12	1.63
23	0.25	-0.59	46	0.00	-0.60

taken, reached the value of 45 tapping (the average tap to tap was 2 h and 30 min).¹⁾

The basic thermal characteristics used in the definition of the various designs proposed throughout the work, following the analysis system proposed by the Nodal Wear Model (NWM), can be made specified *via* three parameters. That is to say, that the model described by criterion M(A; B; C), would represent that configuration for which:

- $A = h_g^{\text{fused}}$, global coefficient of heat transport between the fused (ferroalloy or slag) and the work refractory, in $\text{W} \cdot \text{m}^{-2} \cdot \text{K}^{-1}$.
- $B = \bar{\lambda}_{\text{refractory}}$, average conductivity coefficient of the materials that shape the total thickness of lining furnace, in $\text{W} \cdot \text{m}^{-1} \cdot \text{K}^{-1}$. Bearing in mind that:

$$\bar{\lambda}_{\text{refractory}} = x_o \left(\sum_1^n \left(\frac{x_i}{\lambda_i} \right) \right)^{-1}$$

where, x_i and λ_i are respectively the thickness and the corresponding thermal conductivity of the different materials lining.

- $C = h_g^{\text{chill}}$, global coefficient heat transport in the fluid used (a current chill is forced by air or water) throughout the bottom of the wall-plate, in $\text{W} \cdot \text{m}^{-2} \cdot \text{K}^{-1}$.

It is possible to state therefore that the furnace used for the manufacture of refined ferroalloy that was used until the year 2000, can be defined according to the previously mentioned criteria, such as model M(18; 5.0; 14–19).^{1,3)} In this model, the global heat transport coefficient from point 43 to point 14 of Fig. 1 and Table 1 (steel lover shell of the bottom furnace) towards the air, it takes values between 14 and 19 $\text{W} \cdot \text{m}^{-2} \cdot \text{K}^{-1}$.

The wearing measures, carried out at the end of each tapping in center of the lining bottom furnace (point 1, Fig. 1), were aimed at a chemical wearing mechanism in which the control stage is the diffusion of silicon from the interface

Table 2. Study compared of the characteristics of the five models of operation of an electrical furnace that produces low carbon ferromanganese.

Characteristics	Models Operation Condition				
	M (18;5.0;14-19)	M (60;5.4,18-43)	M (60; 5.4;1200)	M (60;13.5;1200)	M (60;16.2; 1200)
Refractory	Average Conductivity of Materials = 5.0 W·m ⁻¹ ·K ⁻¹	Average Conductivity of Materials = 5.4 W·m ⁻¹ ·K ⁻¹	Average Conductivity of Materials = 5.4 W·m ⁻¹ ·K ⁻¹	Average Conductivity of Materials = 13.5 W·m ⁻¹ ·K ⁻¹	Average Conductivity of Materials = 16.2 W·m ⁻¹ ·K ⁻¹
Coolant for the bottom plate	Air	Air	Water	Water	Water
Furnace life	45 taps	1200 taps	1800 taps	2100 taps	Infinite taps
Remarks	Old model furnace	Model operative today to furnace	Introducing water cooling in the bottom	Non guaranteed self-coated formation	Self-coated with solidified ferromanganese

towards the ferroalloy. The nodal equation of erosion, $(v_{eros})_i$, that adjusts to the experimental dates (45 taps of average, with a speed of wearing down, v_{eros} , of 0.27 cm · h⁻¹), expressed in meters per second, is as follows, **Table 2**^{1,3,4}:

$$(v_{eros})_i = AL^{-1/2} \left(\frac{\Delta\rho_i}{\rho_i} \right)_{Fe-Mn}^{1/6} D_{Si(Fe-Mn)}^{2/3} (\%Si - \%Si^=) \times \left(\frac{\rho_i}{\rho_g^{ref}} \right) \left(\frac{100}{\%cm} \right) \dots\dots\dots(1)$$

where:

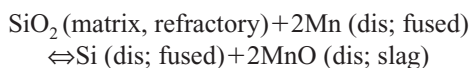
- A : is a constant equal to 8.80 · 10⁻³, with m^{1/6} · s^{-1/3} units.⁴⁾
- L : is a characteristic linear dimension that, in the case of an electric furnace corresponding to model M(18; 5.0; 14–19), would be equal to the arithmetic average of the crucible radius and the height of the metal and the dreg in meters ($L=1.20$ m).
- $\Delta\rho_i$: is the density difference for ferromanganese between nodes adjacent to “ i ” in the work interface fused-refractory (kg · m⁻³).
- ρ_i : is the density of ferromanganese in node “ i ” in the work interface fused-refractory (kg · m⁻³)⁵⁾:

$$\rho_i = 7125 - 0.983T(K)$$

- D_{Si} : is the silicon diffusion coefficient in ferromanganese to the temperature of node “ i ” (m² · s⁻¹)⁵⁾:

$$D_{Si} = 4.50 \cdot 10^{-7} \exp\left(-\frac{4626}{T(K)}\right)$$

- $\%Si$: is the silicon concentration in mass% of the fused (Fe–80%Mn, 1.4% C, 0.15% P) in the case of M(18; 5.0; 14–19) it is equal to 0.80%.
- $\%Si^=$: is the maxima concentration of silicon in mass% (equilibrium concentration) in ferromanganese to the temperature of the node “ i ”. The value of the maximum concentration of silicon concentration is tied to the following thermodynamic balance^{4,6)}:



From the free energies on manganese and silicon oxides

formation and the Raoult activity coefficients of silicon and manganese in the fused ferroalloy, the following expression is reached^{5,6)}:

$$\%Si^= = 32\,000 \exp\left(-\frac{16\,482}{T(K)} + 3.49\right)$$

- ρ_g : is bulk density-mass of basic the monolithic product in contact with the fused (the material reference A, Fig. 1 and Table 1) is 2 100 kg · m⁻³.
- $\%cm$: is the structural factor that expresses the proportion of the matrix component in the monolithic work refractory (the material reference A, Fig. 1 and Table 1) by mass percentage. In model M(18; 5.0; 14–19), $\%cm=0.19\%$.

One of the disadvantages that has characterized model M(18; 5.0; 14–19), has been not knowing how to diligently take advantage of the good properties as opposed to the chemical wearing down of the basic wall-plate of basic monolithic refractory (MgO+CaO=95%) (region A, Fig. 1 and Table 1), due to two fundamental reasons:

- a) The lack of suitable industrial practices at that moment, in order to thermally stabilize the monolithic material before operating the furnace.
- b) Working in a discontinuous manner (to take advantage of the lower costs by using cheaper nocturnal energy rates), with the design represented in Fig. 1 and Table 1, the development of tensions between the work monolithic and the security sintered product were provided, causing the bonding strength (spalling) between the two refractory regions.^{7,8)}

3. Experimental Results

The predictions made by the Nodal Wear Model (NWM) on the possible design alternatives for M(18; 5.0; 14–19) with an improvement in the results in the 100 taps. However, it is necessary to remember that the projections that were carried out were solely supported by changes in the equivalent conductivity of the materials used for the relining furnace (walls and bottom), $\bar{\lambda}_{refractory}$. That is to say, a design with the following characteristics was specifically simulated: M(18; 8.3; 14–19), capable of reaching 100 taps.¹⁾

The true revolution begins when h_g^{fused} and h_g^{chill} values are modified substantially and, to a lesser extent, those for the

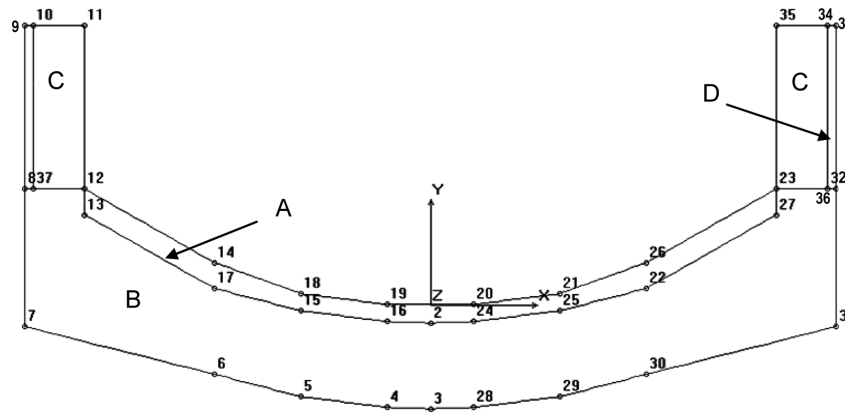


Fig. 2. Chemical, Table 2, geometrical and lining characteristics (regions A; B; C and D) of electric furnace according model M(60; 5.4; 18–43) to producing refined ferromanganese.

Table 3. Chemical (in mass%), geometrical and lining characteristics of electric furnace of the Fig. 2 according model M(60; 5.4; 18–43) to producing refined ferromanganese.

Region A: Magnesia castable refractory (MgO + CaO = 95%; SiO ₂ = 0.60%; Fe ₂ O ₃ = 3.8%; Al ₂ O ₃ = 0.30%) Thickness = 10 cm					
Region B: Brick Magnesia Sintered (dense) Thickness = 50 cm					
Region C: Brick Chrome-Magnesia (dense)					
Region D: Fibber glass (Insulator)					
Point	X coordinate	Y coordinate	Point	X coordinate	Y coordinate
1	0.00	0.00	20	0.25	0.01
2	0.00	-0.10	21	0.75	0.07
3	0.00	-0.60	22	1.25	0.10
4	-0.25	-0.59	23	2.00	0.68
5	-0.75	-0.53	24	0.25	-0.09
6	-1.25	-0.40	25	0.75	-0.03
7	-2.35	-0.12	26	1.25	0.25
8	-2.35	0.68	27	2.00	0.53
9	-2.35	1.63	28	0.25	-0.59
10	-2.30	1.63	29	0.75	-0.53
11	-2.00	1.63	30	1.25	-0.40
12	-2.00	0.68	31	2.35	-0.12
13	-2.00	0.53	32	2.35	0.68
14	-1.25	0.25	33	2.35	1.63
15	-0.75	-0.03	34	2.30	1.63
16	-0.25	-0.09	35	2.00	1.63
17	-1.25	0.10	36	2.30	0.68
18	-0.75	0.07	37	-2.30	0.68
19	-0.25	0.01			

equivalent thermal conductivity of the wall and bottom furnace, $\bar{\lambda}_{refractory}$. When work began, starting in the year 2001, with model M(60; 5.4; 18–43) the description of which is found in Fig. 2 and Table 3, the number of taps increases up to 1200 (Table 2). The modifications in the qualities used are not substantial: a monolithic product of magnesia base (MgO+CaO=95%) is continued to be used as work refractory in bottom furnace. Nevertheless, the improvements which were produced regarding heat transport effectiveness and rapidity from fused ferroalloy towards refractory lining, h_g^{fused} , went from 18 to 60 W·m⁻²·K⁻¹. With these antecedents, the duration of the time tap to tap was reduced remarkably: from 2 h and a half in model M(18; 5.0; 14–19) and to 1 h and 15 min for model M(60; 5.4; 18–43).

Refrigeration at heart of the bottom furnace, h_g^{chill} =18–43 (increase power fan drive), improved substantially although forced airflow as a coolant means is continued to be used. Although the average conductivity of the wall-plate has been increased slightly, $\bar{\lambda}_{refractory}$ =5.4, a important change in strategy exists, however, in the definition of model M(60; 5.4; 18–43):

- The elimination of insulating barriers at bottom: the magnesia sintered bricks contact directly with the furnace’s steel shell, region B of Fig. 2 and Table 3.
- The thickness of the material used for the construction of the work lining (monolithic or casting basic refractory) is divided by into three: for 30.0 cm it becomes 10.0 cm: the thickness region A in the M(18; 5.0; 14–19) is 30.0 cm, Table 1, and to region A in the M(60; 5.4; 18–43) is 10.0 cm, Table 3).

When two materials of different thermal and mechanical characteristics come into contact (thermal conductivity, coefficient of expansion and elasticity module), the development of cracks into separation interface is probable.^{7,8)} The possibility of fracture is greater as the value of the thickness of the monolithic work refractory is increased, $e_{MgO-Cast}$, as well as the following ratio:

$$\frac{e_{MgO-Cast}}{e_{MgO-Bric}}$$

where, $e_{MgO-Bric}$, is the thickness of the sintered magnesia

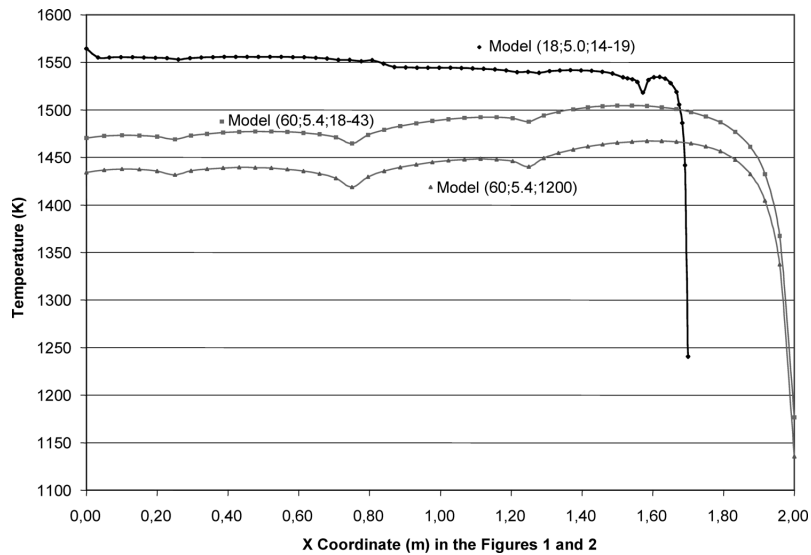


Fig. 3. Profiles of temperature (models M(18; 5.0; 14–19), M(60; 5.4; 18–43) and M(60; 5.4; 1 200), to the beginning of the campaign of working lining furnace, along refractory-fused interface.

brick layer that acts as a security refractory,^{8,9)} region B Fig. 2 and Table 3.

The erosion equation applicable to each of the nodes of the refractory-fused interface in model M(60; 5.4; 18–43), (1) is identified with the equation. Nevertheless, some parameters exist that have been slightly modified with respect to model M(18; 5.0; 14–19):

- The characteristic linear dimension becomes 1.34 ms ($L=1.34$ ms).
- The %cm of the work refractory is 2.50%.
- The specification of silicon in high quality ferromanganese has moved to the area of 0.40%.

In addition to the number of tappings (it can be deemed that after 1 200 taps, Table 2, and with the repairs conducted throughout the work campaign, the work monolithic refractory thickness is found to be totally eliminated due to the chemical wearing mechanism), another of the instruments that validates the erosion equation is by carrying out the calculation of the amount of basic monolithic material ($MgO+CaO=95\%$) used to repair to the differentials wears produced in the lining furnace. By means of application of the NWM, a result of 1 500 kg is reached that coincides with the amounts that are used in industrial activities: the material used for repairs represents 50% of the amount that initially was installed for the construction of the lining furnace, 3 000 kg).

One fundamental hypothesis of NWM, and which justifies the differentials refractory wears that contact with fused, is that by which the speed of erosion, v_{eros} , depends on the node temperature i , T_i , and on the temperature differences that are reached between node, i , and its adjacent node, $i+1$,^{9,10)}:

$$v_{eros} = f(T_i; \Delta T_i) \dots\dots\dots(2)$$

Therefore, one of the design alternatives for stable linings furnace will be to development of those alternatives that reach minimum. T_i . Model M(60; 5.4; 18–43), has meant a decrease by 90°C (90 K) in the maximum temperature reached in model M(18; 5.0; 14–19), Fig. 3. Nevertheless, all the alternatives that can be formulated have to take into

account that the temperature distributions throughout the external steel shell, cannot surpass 350°C (623 K): remember what carbon steels present serious flow problems at temperatures on the order of 550°C (823 K), Fig. 4 (plastic deformations or creep of carbon steel to high temperatures).

4. New Proposals

External refrigeration with water has meant an extraordinary advance in the integrity of metallurgical processes although it has not always been interpreted correctly: in some publications it could be interpreted that the best the refractory for any coating is water.^{9–11)}

Via the use of NWM, it is possible to achieve a suitable quantitative interpretation of the advantages and disadvantages that can lead to the presence of a high capacity coolant means in the coldest area of the refractory coating that connects to the installation’s steel structure.

With the aim of causing a decrease in nodal temperature, T_i (Eq. (2)), in order to improve the yield of model M(60; 5.4; 18–43), it is possible to think about designing external a chill system with water at furnace bottom (from points 7 to 31 in Fig. 2 and Table 2). One would be thinking about model M(60; 5.4; 1 200) in which the external refrigeration attempts to achieve an average decrease in the node temperatures for the refractory-ferro alloy interface at 30°C (30 K), Fig. 3. The projections made with NWM would guarantee, with the same refractory repair consumption during furnace operation, campaign duration of 1 800 taps, Table 2. On the other hand, the temperature in the steel structure at the steel bottom furnace would be approximately 60°C (333 K) (a water temperature restriction is established at 50°C (323 K), Fig. 4.

Another alternative to dramatic diminish node temperatures, T_i , would be to simultaneously act, not only, on the h_g^{chill} values, but also on $\bar{\lambda}_{refractory}$. Respecting a work thickness of 10.0 cm, it is possible to partially or totally consider replacing the security sintered magnesia lining (region B, Fig. 2 and Table 3) with high conductivity carbon (semi-graphite or graphitic) materials.^{4,11–14)}

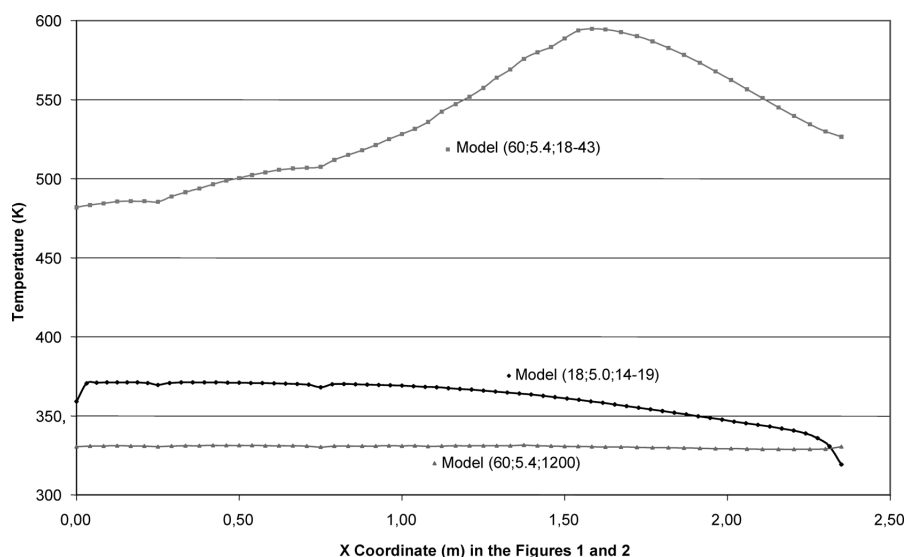


Fig. 4. Profiles of temperature along the chill steel in the bottom furnace for the models M(18; 5.0; 14–19), M(60; 5.4; 18–43) and M(60; 5.4; 1200).

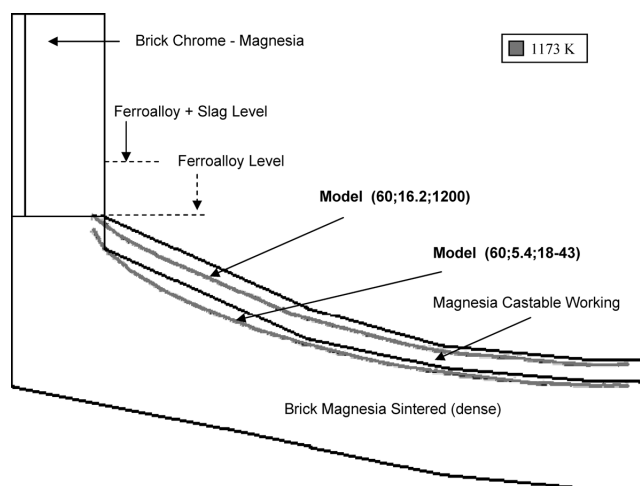


Fig. 5. Situation of the isotherm of 1173 K (900°C) to the beginning of the production campaign for the models M(60; 5.4; 18–43) and M(60; 16.2; 1200).

It is possible to simulate the behavior of the M(60; 13.5; 1200) and M(60; 16.2; 1200) alternatives in which a remarkable decrease in node temperatures, T_i , in the interface would be achieved. The objective is to obtain, before the 10.0 cm of the work refractory is entirely worn away, the temperatures throughout the refractory-fused interface that do not surpass the temperature which corresponds to ferroalloy solidus temperature, T_{solidus} (in mass%: 80% Mn; 1.40% C; 0.80% Si; 0.15% P and 17.65% Fe). In agreement with the available data, the low carbon ferromanganese temperature would be $T_{\text{solidus}} = 900^\circ\text{C}$ (1173 K).¹⁾

One idea of how the models could work would be *via* the 1173 K (900°C) and 973 K (700°C) isotherms situations, at the beginning of the campaign, **Figs. 5** and **6**. Only in model M(60; 16.2; 1200) do the 973 K (700°C) and 1173 K (900°C) isotherms locate within the work refractory region (the region A, Fig. 2 and Table 3). However, as the wearing down/erosion process proceeds, the nodal temperature distribution in the refractory-fused interface as well as the relative position of the isotherms within the

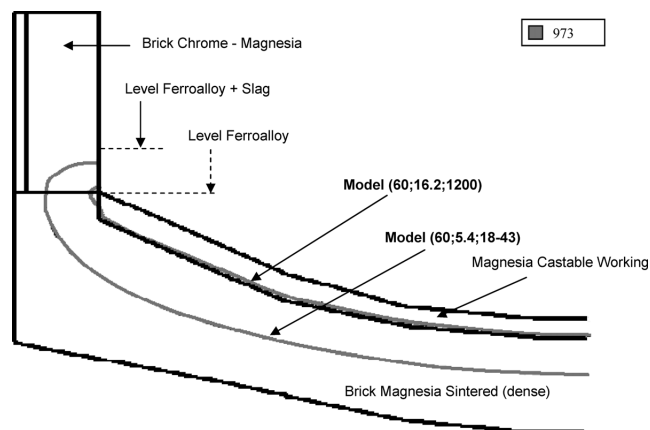


Fig. 6. Situation of the isotherm of 973 K (700°C) to the beginning of the production campaign for the models M(60; 5.4; 18–43) and M(60; 16.2; 1200).

wall-plate become altered.

However, it would be possible to simulate the distribution of nodal temperatures that could be achieved when the work lining has been uniformly worn away and only has 1.0 cm of refractory remaining. As can be seen in **Fig. 7**, model M(60; 16.2; 1200) is the only one that can reach interfaces temperatures below 1173 K (900°C). It is possible to provoke what is known in metallurgy as “cold wall and bottom” or “self coating”, Table 2. This solution would allow work to be carried out in the furnace employing a number of tappings that would be practically indefinite, unless a perforation or crack were present in the refractory lining due to causes other than the chemical erosion mechanism (spalling and thermal shock).⁴⁾

5. Conclusions

NWM has proven itself to be an effective instrument for the study and simulation of the erosion fluid processes that make contact with high temperatures refractory. This mission not only has been developed successfully in the scope of the ferroalloy and the electrical furnace, but has also

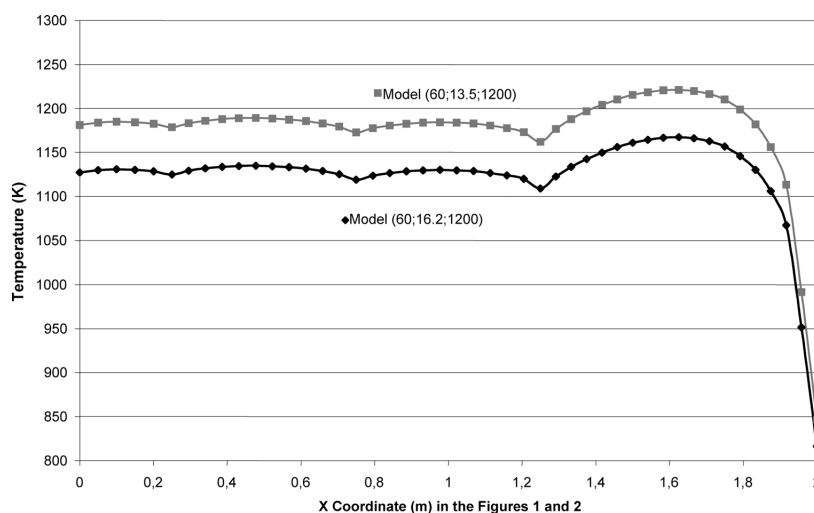


Fig. 7. Profiles of temperature, when an uniform wear of 9.0 cm of the region A Fig. 2, has been produced along the interface castable refractory work with the fused for the models M(60; 13.5; 1200) and M(60; 16.2; 1200).

been applied to other equipment and metallurgical systems (blast furnaces; copper converters, hot metal transport car).

The most novel and interesting aspect of this work is observing how new designs can be projected using NWM that have not yet been experimentally accredited. Under this hypothesis, a new design for a furnace, M(60; 16.2; 1200), that can produce refined ferromanganese is proposed which is capable of working with a solidified metal, “self coating” (ferroalloy) on a security refractory.

Acknowledgements

The authors of this work wish to thank the Ferroatlántica Group (F. Fenández; J. C. Sánchez and J. Bullón), Ministry of Education and Science-Spain (MEC): MAT2003-00502 as well as the Ministry of Foreign Affairs and Cooperation (MAEC): MAEC-AECI- B/1629/04; B/2884/05; B/5814/06 and B/7648/07 for the assistance and collaboration provided by them in order to carry out this work.

REFERENCES

- 1) L. F. Verdeja, R. Parra, J. P. Sancho and J. Stud: *ISIJ Int.*, **43** (2003), 192.
- 2) H. Cengizler and R. H. Eric: *Steel Res. Int.*, **77** (2006), No. 11, 793.
- 3) R. Parra, J. Mochón, R. Martín, J. I. Verdeja, M. F. Barbés, L. F. Verdeja, N. Kanari and I. Ruíz-Bustinza: *Ironmaking Steelmaking*, **36** (2009), No. 7, 529.
- 4) L. F. Verdeja, J. P. Sancho and A. Ballester: *Refractories and Ceramics Materials, Síntesis*, Madrid, España, (2008), 156, 294.
- 5) The Japan Society for Promotion of Science: 19th Committee on Steelmaking 1988, *Steelmaking Data Sourcebook*, Gordon and Breach Science Publishers, Montreux, Switzerland, (1988), 278.
- 6) J. P. Sancho, L. F. Verdeja and A. Ballester: *Extractive Metallurgy: Processes of Obtaining, Synthesis*, Madrid, España, (2000), 33.
- 7) C. Marcos, I. Rodríguez, M. F. Barbés and L. F. Verdeja: *Bol. Soc. Esp. Ceram. V.*, **48** (2006), No. 5, 243.
- 8) Ch. Goñi, M. F. Barbés, V. Bazán, E. Brandaleze, R. Parra and L. F. Verdeja: *J. Ceram. Soc. Jpn.*, **114** (2006), No. 8, 665.
- 9) R. Parra, L. F. Verdeja, M. F. Barbés, Ch. Goñi and V. Bazán: *JOM*, **57** (2005), No. 10, 29.
- 10) L. F. Verdeja, M. F. Barbés, R. González, G. A. Castillo and R. Colás: *Rev. Metal. Madrid*, **41** (2005), No. 6, 449.
- 11) M. F. Barbés, É. Marinas, E. Brandaleze, R. Parra, L. F. Verdeja, G. A. Castillo and R. Colás: *ISIJ Int.*, **48**, (2008), No. 2, 134.
- 12) L. F. Verdeja, R. Parra, M. F. Barbés, Ch. Goñi and V. Bazán: *Steel Grips*, **3** (2005), No. 2, 105.
- 13) J. P. Bennett and J. D. Smith: *Fundamentals of Refractory Technology: Corrosion industrial refractories*, The American Ceramic Society, Ohio, EE.UU., (2001), 135.
- 14) R. A. McCauley: *Corrosion of Ceramics*, Marcel Dekker, Nueva York, EE.UU. (1995), 8